



Sauter mean diameter determination for the fine fraction of suspended sediments using a LISST-25X diffractometer

Leonardo Filippa*, Alfredo Trento, Ana M. Álvarez

Facultad de Ingeniería y Ciencias Hídricas, Universidad Nacional del Litoral, CC 217, 3000 Santa Fe, Argentina

ARTICLE INFO

Article history:

Received 12 July 2011

Received in revised form 4 November 2011

Accepted 15 November 2011

Available online 22 November 2011

Keywords:

Sauter mean diameter

Fine fraction

LISST-25X

Granulometric composition

ABSTRACT

The LISST-25X ability for measuring the Sauter mean diameter of the fine fraction of sediment samples, SMD_f is evaluated. A simple algorithm to determine the SMD_f is proposed. The algorithm is based on the standard output variables from the LISST-25X diffractometer: Sauter mean diameter of the complete sample, SMD_t ; Sauter mean diameter of the coarse fraction, SMD_g ; total suspended sediment concentration, SSC_t , and coarse suspended sediment concentration, SSC_g . Validation is performed in the laboratory by contrasting algorithm results from complete sediment samples against LISST SMD_t measurements made on the fine fraction of the samples. A second validation is performed by comparison between algorithm results and Malvern measurements on the same samples. The samples are from the Salado River (Argentina) and the Paraná River (Argentina). Their SMD_t range from 10 μm to 70 μm .

Results indicate that the algorithm determines the Sauter mean diameter of the fine fraction in a reliable way, with average differences of 1.4 μm (algorithm-LISST comparison) and 3.4 μm (algorithm-Malvern comparison). The observed differences are attributed to operational conditions rather than to algorithm limitations. A correlation between calculated SMD_f and d_{50} of the fine fraction is also established, with a determination coefficient of $R^2 = 0.46$.

© 2011 Elsevier Ltd. All rights reserved.

1. Introduction

The Sauter mean diameter (SMD), also known as Surface Area Moment Mean, $D(3,2)$ [1], or d_{32} , estimates the mean size of a given particle distribution. It is defined as the diameter of a sphere that has the same volume/surface area ratio as the particle of interest. Mathematically, SMD is defined according to Eq. (1) [2]:

$$SMD = d_{32} = \frac{\int_{d_{min}}^{d_{max}} d^3 p(d) dd}{\int_{d_{min}}^{d_{max}} d^2 p(d) dd} \quad (1)$$

where d indicates the particle diameter, d_{max} and d_{min} indicates the maximum and minimum diameters of the particle

distribution, $p(d)$ indicates the probability density function of d size.

The LISST-25X is a diffractometer from the LISST series of instruments developed by Sequoia Scientific, Inc. It features a submersible laser sensor designed for *in situ* as well as laboratory measurements of SMD of the complete (i.e. original) sample (SMD_t), SMD of the coarse fraction (SMD_g), total suspended sediment concentration (SSC_t), coarse suspended sediment concentration (SSC_g), optical transmission level (TO), and operating depth. The LISST-25X operates within a concentration range of 0.10–1000 mg/L; it detects mean diameters at the 2.50–500 μm interval, and from 63 to 500 μm for coarse sediments, with a TO range between 30% and 98%. Its optical sensor includes a 670 nm wavelength laser, with optical path length of 2.50 cm [3]. Its operating principle is based on the small-angle forward laser light scattering theory proposed by Lorenz–Mie [4]. More detailed information about the optical sensor operating

* Corresponding author.

E-mail address: leofi2004@yahoo.com.ar (L. Filippa).

principle and the equations that connect this theory to the concentration and diameter determinations can be found in [5].

The Malvern Mastersizer 2000 is a diffractometer broadly used in laboratory work. The size range measured by Malvern runs from 0.02 to 2000 μm. Besides measuring SMD, it determines the granulometric composition of the samples. Some applications for sediment size determinations using this diffractometer can be found elsewhere [6,7].

Determination of suspended sediment sizes is a basic concern in any study of sediment transport. LISST-25X, by means of SMD_t and SMD_g , provides information about mean size of the total and the coarse fraction of suspended sediments, respectively. Nevertheless, no direct determination is made on the fine fraction of sediments. Several studies have shown the fine sediments to be responsible for the transport of pollutants in water bodies [8–10]. Thus, to have an estimation of the size of fine fraction might be critical in such cases.

In a previous work [11] a laboratory evaluation of LISST-25X has been made. A comparison between LISST-25X SMD_t and Malvern SMD determinations was presented. Those results indicated good agreement between SMD determinations from both diffractometers (being the determination coefficient $R^2 = 0.98$). It has also been established a correlation between LISST SMD_t and d_{50} (median diameter) of the samples, which is the most commonly used diameter in hydraulic and maritime engineering. However, LISST-25X determinations of the fine fraction had not yet been evaluated.

The aim of this work is to evaluate the ability of the LISST-25X diffractometer for measuring the Sauter mean diameter of the fine fraction of sediments. As stated above, SMD_f is not an output variable from LISST-25X, therefore a simple algorithm for its calculation is validated here. The algorithm is based on the output variables from the LISST-25X: SMD_t , SMD_g , SSC_t and SSC_g . The second objective of this work is to establish a correlation between SMD_f and d_{50} of the fine fraction.

Different samples of natural sediments from the Salado River and the Paraná River (both Rivers from Argentina) are tested. Validation is made by comparison between algorithm results from the complete samples and LISST and Malvern measurements made on the fine fraction of the samples.

The results of this work aim to broaden LISST-25X capabilities, enabling the instrument to provide, also, explicit information on the fine fraction of suspended sediments.

2. Materials and methods

2.1. Algorithm for the SMD_f estimation

The LISST-25X instrument estimates the SMD_t based on Eq. (2) [5]:

$$SMD_t = 1.5 \frac{SSC_t^V}{SSC_t^{sup}} \quad (2)$$

where SSC_t^V is the total particle volume concentration, and SSC_t^{sup} represents the total particle surface area concentration. Considering that for coarse and fine fractions, the ratio

of Eq. (2) can be applied, the following relations may be obtained: $SSC_g^{sup} = 1.5SSC_g^V/SMD_g$ and $SSC_f^{sup} = 1.5SSC_f^V/SMD_f$; where SSC_g^{sup} and SSC_f^{sup} indicate the coarse and fine particle surface area concentrations; SSC_g^V and SSC_f^V indicate the coarse and fine particle volume concentrations; SMD_g and SMD_f indicate Sauter mean diameters for coarse and fine fractions, respectively. Assuming that $SSC_t^{sup} = SSC_g^{sup} + SSC_f^{sup}$, the following equation for the SMD_f may be obtained:

$$SMD_f = \frac{SSC_f^V}{\frac{SSC_t^V}{SMD_t} - \frac{SSC_g^V}{SMD_g}} = \frac{SSC_t^V - SSC_g^V}{\frac{SSC_t^V}{SMD_t} - \frac{SSC_g^V}{SMD_g}} \quad (3)$$

Note that SSC_t^V , SMD_t , SSC_g^V , SMD_g are all output variables from the LISST-25X instrument. Eq. (3) may be expressed as:

$$\begin{aligned} SMD_f &= 1.5SSC_f^V / (SSC_t^{sup} - SSC_g^{sup}) \\ &= 1.5(SSC_t^V - SSC_g^V) / (SSC_t^{sup} - SSC_g^{sup}) \end{aligned}$$

It should be noted that in case of absence of coarse sediments in the suspension, both SSC_g^V and SSC_g^{sup} are equal zero, then $SMD_f = SMD_t$.

2.2. Propagation of error in algorithm results

The error propagation in Eq. (3) will be approached following Eq. (4) for the uncertainty in a function of several variables [12]:

$$\Delta SMD_f = \sqrt{\left(\frac{\partial SMD_f}{\partial SSC_t^V} \Delta SSC_t^V\right)^2 + \left(\frac{\partial SMD_f}{\partial SSC_g^V} \Delta SSC_g^V\right)^2 + \left(\frac{\partial SMD_f}{\partial SMD_t} \Delta SMD_t\right)^2 + \left(\frac{\partial SMD_f}{\partial SMD_g} \Delta SMD_g\right)^2} \quad (4)$$

where ΔSMD_f is the error propagation in the SMD_f equation; ΔSSC_t^V , ΔSSC_g^V , ΔSMD_t and ΔSMD_g are the errors for SSC_t^V , SSC_g^V , SMD_t and SMD_g , respectively (all of them approximated by the corresponding standard deviations); and the partial derivatives of SMD_f : $\frac{\partial SMD_f}{\partial SSC_t^V}$, $\frac{\partial SMD_f}{\partial SSC_g^V}$, $\frac{\partial SMD_f}{\partial SMD_t}$ and $\frac{\partial SMD_f}{\partial SMD_g}$, being obtained from Eq. (3). For the sake of simplicity the development of derivatives is not presented here.

2.3. Granulometric composition of the samples and laboratory tests

Field samples were collected from the Salado and Paraná Rivers; once in the laboratory, the samples were air dried and then homogenized in a mortar. Finally, they were sieved using a 2 mm plastic sieve in order to remove major detritus. The fine fraction was then obtained by dry sieving of the complete samples using an ASTM 230 sieve.

The tested samples, their source and granulometric composition are presented in Table 1. The granulometric composition was obtained with a Malvern Mastersizer 2000 diffractometer. The samples are divided into two groups (see Table 1): complete samples (samples #1–8), mainly composed of coarser material with a significant proportion of medium and coarse silt particles; and fine fraction (samples #9–15) corresponding to the fine fraction of the complete samples. Further information about

Table 1

List of tested samples, source and granulometric composition obtained with Malvern Mastersizer. E1 (sample #16), not belonging to the defined groups, is shown as a reference.

| # | Sample | Source | Clay $d < 2$ (%) | Very fine silt $2 < d < 8$ (%) | Fine silt $8 < d < 16$ (%) | Mean silt $16 < d < 32$ (%) | Coarse silt $32 < d < 63$ (%) | Very fine sand $63 < d < 125$ (%) | Fine to very coarse sand $125 < d < 250$ (%) | Bi-modal |
|----|--------|--|------------------------|--------------------------------------|----------------------------------|-----------------------------------|-------------------------------------|---|--|----------|
| 1 | S25b | Suspended sediments, Salado River | 3.8 | 9.7 | 9.6 | 23.2 | 15.5 | 22.1 | 16.1 | Yes |
| 2 | S29 | Suspended sediments, Salado River | 0.6 | 3.1 | 4.5 | 24.7 | 21.1 | 24.6 | 21.4 | Yes |
| 3 | S36 | Suspended sediments, Salado River | 0.8 | 5.8 | 7.5 | 22.7 | 15.6 | 26.4 | 21.2 | Yes |
| 4 | S28a | Suspended sediments, Salado River | 0.6 | 3.2 | 4.4 | 20.9 | 21.2 | 35.0 | 14.7 | Yes |
| 5 | S28b | Suspended sediments, Salado River | 0.6 | 3.3 | 4.6 | 20.9 | 19.3 | 31.7 | 19.6 | Yes |
| 6 | S37OR | Suspended sediments, Salado River | 1.4 | 6.7 | 6.1 | 17.2 | 15.0 | 38.1 | 15.5 | No |
| 7 | SP1 | Bed sediments, Parana River (75% PR); suspended sediments, Salado River (25% S37F) | 0.6 | 3.3 | 3.2 | 9.9 | 8.7 | 10.3 | 64.0 | Yes - S |
| 8 | SP2 | Bed sediments, Parana River (90% PR); suspended sediments, Salado River (10% S37F) | 0.3 | 2.1 | 1.9 | 5.6 | 5.0 | 7.4 | 77.7 | Yes - S |
| 9 | S25bF | Suspended sediments, Salado River | 6.0 | 13.1 | 12.8 | 32.3 | 21.5 | 14.3 | 0.0 | No |
| 10 | S36F | Suspended sediments, Salado River | 1.6 | 13.1 | 14.7 | 33.2 | 21.9 | 15.4 | 0.1 | No |
| 11 | S37F | Suspended sediments, Salado River | 2.2 | 9.5 | 9.6 | 29.7 | 25.6 | 23.4 | 0.0 | No |
| 12 | S28bF | Suspended sediments, Salado River | 4.9 | 8.6 | 9.5 | 33.2 | 26.2 | 17.6 | 0.0 | No |
| 13 | S28aF | Suspended sediments, Salado River | 1.2 | 7.2 | 7.6 | 31.5 | 29.7 | 22.8 | 0.0 | No |
| 14 | S29F | Suspended sediments, Salado River | 1.0 | 4.7 | 5.1 | 32.4 | 32.8 | 23.9 | 0.1 | No |
| 15 | E2 | Glass (25–32 μm) | 0.0 | 0.0 | 0.0 | 98.0 | 2.0 | 0.0 | 0.0 | No |
| 16 | E1 | Glass (72–90 μm) | 0.0 | 0.0 | 0.0 | 0.0 | 0.0 | 100.0 | 0.0 | No |

Note: The d letter represents the size in microns. The samples labeled with the F letter were previously sieved using an ASTM 230 sieve. Yes-S: means strongly bi-modal.

the tested samples can be found in [11]. The granulometric distribution of E12 sample (being composed of 50% from E1 +50% from E2) was not determined. Instead the composition of E1 (sample #16) and E2 are shown in Table 1.

All the tests with LISST-25X were performed using the following measurement protocol:

- Preparation of 100 mg/L and 200 mg/L concentrations for each sample in the tests chamber of the LISST instrument, with 1336.50 mL of distilled water and 13.50 mL of 4% sodium hexametaphosphate as a dispersant agent [13].
- Forty measurements of SMD_t , SMD_g , SSC_t , SSC_g , TO per every concentration at 5-s intervals.
- Continuous stirring of the water using a manual stirrer.
- All tests were performed at constant environment light and temperature (25 °C) conditions.

3. Results

Table 2 summarizes the major results of the tested samples. It shows the corresponding LISST-25X determinations: mean sizes (SMD_t , SMD_g), mean concentration values (SSC_t , SSC_g , SSC_g/SSC_t) and variation coefficients (VC); the algorithm results: calculated SMD_f (for complete samples) and error propagation of SMD_f ; and the results using Malvern Mastersizer: SMD , coarse particle content. The coarse particle content is obtained from Table 1 by adding the sand percentages and converting them to relative units (i.e. from 0 to 1).

A comparison between calculated SMD_f and LISST SMD_t measurements made on the fine fraction is presented in

Fig. 1. Most samples show good agreement between the calculated values and those measured in the fine fraction. The average difference was 1.4 μm . In general, a slight tendency to underestimations in the algorithm results can be observed.

Fig. 2 contrasts the calculated SMD_f with the measured SMD using the Malvern diffractometer in the fine fraction of the samples. The average observed difference was 3.4 μm . There is also some trend to underestimations in algorithm results when compared to Malvern results.

It must be noted that LISST instrument values are informed using an integer number considering its corresponding resolution (1 μm), whereas Malvern results are informed with two decimals according to its resolution (0.01 μm).

Regarding error propagation, Table 2 shows that it is of the same order than the errors for the rest of the variables and approximately homogeneous for the majority of the samples, except for the SP1 and SP2 samples, where it is an order of magnitude higher. In general the relative error for each measured variable, (being represented by the variation coefficient VC) is the biggest for SSC_g being followed by the errors associated to SMD_f , SMD_g , SSC_t and SMD_t , respectively.

A correlation between algorithm SMD_f and Malvern d_{50} of the fine fraction is presented in Fig. 3. The determination coefficient was $R^2 = 0.46$, being $d_{50} = 2.47 SMD_f$.

As regards the three samples presenting strong bimodality: SP1, SP2 and E12, it is expected that the d_{50} will not be representative of the characteristic size, because for bimodal populations the two modes will be better parameters than the median diameter. Therefore those samples were excluded from the correlation. Besides when including them the correlation was considerably weak.

Table 2

List of results using LISST-25X: mean sizes (SMD_t , SMD_g), mean concentration values (SSC_t , SSC_g , SSC_g/SSC_t), variation coefficients (VC), calculated SMD_f (for complete samples) and error propagation of SMD_f ; and results using Malvern Mastersizer: SMD , coarse particle content.

| Sample | LISST-25X | | | | | | | | | | | Malvern Mastersizer | | |
|--------|---------------------------|-----------|----------------|-----------|---------------------------|-----------|---------|-----------|---------------|---------------------------|--|------------------------|-------------------------|-------------------------|
| | SMD_t (μm) | $VCSMD_t$ | SSC_t (mg/L) | $VCSSC_t$ | SMD_g (μm) | $VCSMD_g$ | SSC_g | $VCSSC_g$ | SSC_g/SSC_t | SMD_f (μm) | ΔSMD_f Eq. (4) (μm) | $\Delta SMD_f / SMD_f$ | SMD (μm) | Coarse particle content |
| S25b | 16 | 0.07 | 118.1 | 0.07 | 93 | 0.16 | 28.6 | 0.31 | 0.24 | 13 | 1.4 | 0.11 | 10.64 | 0.38 |
| S29 | 27 | 0.07 | 211.6 | 0.08 | 111 | 0.11 | 69.0 | 0.21 | 0.32 | 20 | 2.2 | 0.11 | 31.28 | 0.46 |
| S36 | 16 | 0.11 | 191.5 | 0.11 | 110 | 0.18 | 54.5 | 0.38 | 0.28 | 12 | 2.2 | 0.18 | 24.20 | 0.48 |
| S28a | 20 | 0.09 | 172.0 | 0.11 | 97 | 0.14 | 51.0 | 0.31 | 0.29 | 15 | 2.3 | 0.15 | 31.34 | 0.50 |
| S28b | 21 | 0.11 | 121.4 | 0.14 | 113 | 0.19 | 42.7 | 0.41 | 0.34 | 15 | 3.5 | 0.23 | 31.48 | 0.51 |
| S37OR | 16 | 0.12 | 156.4 | 0.16 | 86 | 0.28 | 46.6 | 0.30 | 0.29 | 12 | 2.1 | 0.18 | 12.24 | 0.54 |
| SP1 | 37 | 0.16 | 983.4 | 0.26 | 234 | 0.08 | 754.5 | 0.25 | 0.77 | 9 | 11.2 | 1.21 | 42.37 | 0.74 |
| SP2 | 57 | 0.25 | 154.4 | 0.34 | 235 | 0.11 | 138.6 | 0.37 | 0.89 | 7 | 32.1 | 4.71 | 66.96 | 0.85 |
| E12 | 46 | 0.07 | 58.8 | 0.10 | 137 | 0.08 | 32.8 | 0.19 | 0.55 | 25 | 5.9 | 0.24 | N/D | N/D |
| S25bF | 13 | 0.05 | 139.9 | 0.06 | 53 | 0.42 | 11.0 | 0.61 | 0.08 | - | - | - | 7.45 | 0.14 |
| S36F | 13 | 0.09 | 107.6 | 0.11 | 59 | 0.57 | 7.6 | 0.63 | 0.07 | - | - | - | 13.78 | 0.15 |
| S37F | 9 | 0.04 | 270.7 | 0.05 | 25 | 0.36 | 10.2 | 0.44 | 0.04 | - | - | - | 8.43 | 0.23 |
| S28bF | 15 | 0.03 | 263.6 | 0.03 | 62 | 0.16 | 27.8 | 0.21 | 0.11 | - | - | - | 9.10 | 0.17 |
| S28aF | 17 | 0.03 | 256.4 | 0.05 | 71 | 0.13 | 35.3 | 0.21 | 0.14 | - | - | - | 19.09 | 0.22 |
| S29F | 19 | 0.06 | 210.2 | 0.08 | 75 | 0.13 | 32.4 | 0.27 | 0.15 | - | - | - | 22.91 | 0.24 |
| E2 | 26 | 0.08 | 94.6 | 0.14 | 315 | 2.92 | 7.0 | 1.46 | 0.07 | - | - | - | 29.00 | 0.00 |

Note: N/D means no data.

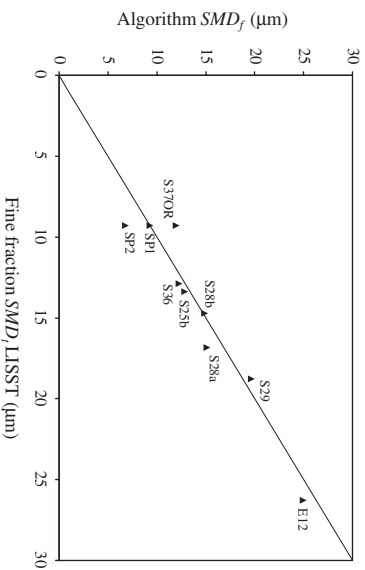


Fig. 1. Calculated SMD_f for complete samples vs. SMD_f measured (LISST instrument in fine fraction).

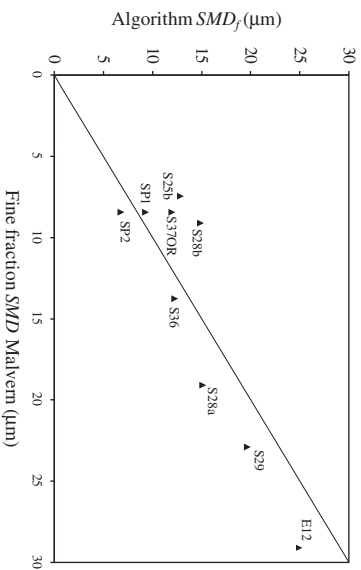


Fig. 2. Calculated SMD_f for complete samples vs. SMD measured (Malvern diffractometer in fine fraction).

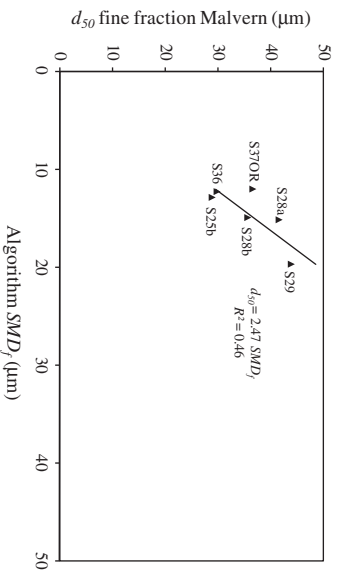


Fig. 3. Algorithm SMD_f – Malvern d_{50} correlation.

4. Discussion

Results show good agreement between algorithm results and measurements made on the fine fraction by LISST and Malvern diffractometers. A slight trend to underestimations in the algorithm calculations is observed, being the differences higher when comparing with Malvern results. Some considerations should be highlighted, when interpreting those differences:

- All of the fine samples had a considerable amount (see Tables 1 and 2) of coarse material: from 14% to 24% for Malvern data and from 4% to 15% for LISST data. Therefore LISST and Malvern measurements were made on fine samples that were not actually “fine samples”. Hence both diffractometers were measuring coarse particles (in the fine samples) that generated some deviations in the measured SMD .
- Malvern instrument stirs the water at much higher velocities than the ones that could be achieved in the tests chamber of the LISST. Hence the possibility of measuring coarse particles is higher for the Malvern instrument (note that the average coarse particle content recorded by Malvern for the fine samples were twice the ones reported by LISST). This could explain why deviations in algorithm results are more pronounced in the comparison with Malvern results.
- In the other hand, algorithm results (see Eq. (3)) are sensitive to all the measured variables: SMD_t , SMD_g , SSC_t and SSC_g ; which are strongly influenced by agitation conditions and the amount of sample being detected by the sensor. This may yield some additional dispersion in the measured data.

The error propagation shows that the errors in the algorithm are approximately homogeneous and of the same order than the errors for the rest of the variables, being all the VC less than unity. The exception occurs for SP1 and SP2 samples where the error becomes considerably higher. These samples have comparatively higher VC for SMD_t and SSC_t which then propagate to the SMD_f results. Those higher VC could be attributed to the high content of coarse material in SP1 and SP2 samples (see Table 1), whose influence on VC had been assessed in [11].

In spite of the differences between algorithm results and the measured data, it is noteworthy the algorithm capability to correctly estimate the SMD_f .

As regards the correlation between SMD_f and d_{50} , it should be pointed out that it is only applicable to sediment samples presenting similar size distributions to those of the tested samples.

5. Conclusions

The results indicate that it has been possible to develop a simple algorithm to determine, in a reliable way, the Sauter mean diameter for the fine fraction of suspended sediments using the information obtained from a LISST-25X sensor. A correlation between algorithm SMD_f and d_{50} of the fine fraction was established, allowing the algorithm results to be implemented in a first estimation of a d_{50} of the fine fraction. This correlation is only applicable

to sediment samples presenting similar size distributions to those of the tested samples.

The average difference observed between the calculated SMD_f for the complete samples and the SMD_t measured with LISST for the fine samples was 1.4 μm . In addition, the average difference observed between the calculated SMD_f and the SMD measured with Malvern was 3.4 μm . Those differences were attributed to the presence of coarse particles in the fine samples and the agitation and sampling conditions, which are considered as operational factors rather than algorithm limitations.

New laboratory tests will be addressed in order to broaden the SMD_t and concentration intervals under which the algorithm is validated.

Acknowledgments

This work was financed by Universidad Nacional del Litoral (UNL) and Agencia Nacional de Promoción Científica y Tecnológica (ANPyCT), grant PICT 35885 to Dr. Alfredo Trento.

References

- [1] A. Rawle, Basic Principles of Particle Size Analysis, Malvern Instruments Online Applications Library, 2010. <[http://www.malvern.com/malvern/kbase.nsf/allbyno/KB000021/\\$file/Basic_principles_of_particle_size_analysis_MRK034-low_res.pdf](http://www.malvern.com/malvern/kbase.nsf/allbyno/KB000021/$file/Basic_principles_of_particle_size_analysis_MRK034-low_res.pdf)>.
- [2] A.W. Pacek, C.C. Man, A.W. Nienow, On the Sauter mean diameter and size distribution in turbulent liquid/liquid dispersions in a stirred vessel, Chem. Eng. Sci. 53 (11) (1998) 2005–2011.
- [3] Sequoia Scientific Inc., LISST-25X Suspended Sediment Sensor Operating Manual, Sequoia Sci Inc, Bellevue (WA), 2008, p. 31.
- [4] Sequoia Scientific, Operating Principle of the LISST-25 Constant Calibration Sediment Sensor, Sequoia Scientific's Online Library, 2008. <<http://sequoiasci.com/Articles/ArticlePage.aspx?pagel=129>>.
- [5] Y.C. Agrawal, O.A. Mikkelsen, Shaped focal plane detectors for particle concentration and mean size observations, Opt. Express 17 (25) (2009) 23066–23077.
- [6] K.R. Dyer, A.J. Manning, Observation of the size, settling velocity and effective density of flocs, and their fractal dimensions, J. Sea Res. 41 (1999) 87–95.
- [7] F. Mietta, C. Chassagne, J.C. Winterwerp, Shear-induced flocculation of a suspension of kaolinite as function of pH and salt concentration, J. Colloid Interface Sci. 336 (2009) 134–141.
- [8] R.J. Gibbs, Effect of natural organic coatings on the coagulation of particles, Environ. Sci. Technol. 17 (4) (1983) 237–240.
- [9] K.G. Taylor, P.N. Owens, R.J. Batalla, C. Garcia, Sediment and contaminant sources and transfers in river basins, in: P.N. Owens (Ed.), Sustainable Management of Sediment Resources: Sediment Management at the River Basin Scale, Elsevier, Oxford, UK, 2008, pp. 83–135.
- [10] W. Lick, Sediment and Contaminant Transport in Surface Waters, CRC Press, Boca Raton, US, 2009.
- [11] L. Filippa, L. Freyre, A. Trento, A. Alvarez, M. Gallo, S. Vinzon, Laboratory evaluation of two LISST-25X using river sediments, Sediment. Geol. 238 (2011) 268–276.
- [12] J.R. Taylor, An Introduction to Error Analysis, the Study of Uncertainties in Physical Measurements, University Science Books, Sausalito, US, 1997.
- [13] H.P. Guy, Laboratory procedures, in: V. Vanoni (Ed.), Sedimentation Engineering, ASCE, New York, 1975, pp. 401–428.